



Neuroimaging Examination of Driving Mode Switching Corresponding to Changes in the Driving Environment

Ryu Ohata^{1*}, Kenji Ogawa² and Hiroshi Imamizu^{1,3,4*}

¹ Department of Psychology, Graduate School of Humanities and Sociology, The University of Tokyo, Tokyo, Japan,

² Department of Psychology, Graduate School of Humanities and Human Sciences, Hokkaido University, Sapporo, Japan,

³ Cognitive Mechanisms Laboratories, Advanced Telecommunications Research Institute International (ATR), Kyoto, Japan,

⁴ Research Into Artifacts, Center for Engineering, The University of Tokyo, Tokyo, Japan

OPEN ACCESS

Edited by:

Belén Rubio Ballester,
Institute for Bioengineering
of Catalonia (IBEC), Spain

Reviewed by:

Otto Lappi,
University of Helsinki, Finland
Isao Nambu,
Nagaoka University of Technology,
Japan

*Correspondence:

Ryu Ohata
ryu.oohata@gmail.com
Hiroshi Imamizu
imamizu@gmail.com

Specialty section:

This article was submitted to
Motor Neuroscience,
a section of the journal
Frontiers in Human Neuroscience

Received: 03 October 2021

Accepted: 31 January 2022

Published: 18 February 2022

Citation:

Ohata R, Ogawa K and
Imamizu H (2022) Neuroimaging
Examination of Driving Mode
Switching Corresponding to Changes
in the Driving Environment.
Front. Hum. Neurosci. 16:788729.
doi: 10.3389/fnhum.2022.788729

Car driving is supported by perceptual, cognitive, and motor skills trained through continuous daily practice. One of the skills that characterize experienced drivers is to detect changes in the driving environment and then flexibly switch their driving modes in response to the changes. Previous functional neuroimaging studies on motor control investigated the mechanisms underlying behaviors adaptive to changes in control properties or parameters of experimental devices such as a computer mouse or a joystick. The switching of multiple internal models mainly engages adaptive behaviors and underlies the interplay between the cerebellum and frontoparietal network (FPN) regions as the neural process. However, it remains unclear whether the neural mechanisms identified in previous motor control studies also underlie practical driving behaviors. In the current study, we measure functional magnetic resonance imaging (fMRI) activities while participants control a realistic driving simulator inside the MRI scanner. Here, the accelerator sensitivity of a virtual car is abruptly changed, requiring participants to respond to this change flexibly to maintain stable driving. We first compare brain activities before and after the sensitivity change. As a result, sensorimotor areas, including the left cerebellum, increase their activities after the sensitivity change. Moreover, after the change, activity significantly increases in the inferior parietal lobe (IPL) and dorsolateral prefrontal cortex (DLPFC), parts of the FPN regions. By contrast, the posterior cingulate cortex, a part of the default mode network, deactivates after the sensitivity change. Our results suggest that the neural bases found in previous experimental studies can serve as the foundation of adaptive driving behaviors. At the same time, this study also highlights the unique contribution of non-motor regions to addressing the high cognitive demands of driving.

Keywords: car driving, motor control, internal model, frontoparietal network, default mode network, salience network

INTRODUCTION

A car is one of the most advanced devices humans operate in daily life. Accordingly, people need to accumulate a certain amount of driving experience to acquire practical driving skill. One of the skills that characterize experienced drivers is the ability to rapidly detect changes in the driving environment and then flexibly switch the driving mode in response to those changes. For example,

experienced drivers can maintain their car's movement at a constant speed regardless of running uphill or downhill, and they can keep their driving stable after their car suddenly encounters a slippery road surface. Such adaptive driving behaviors are supported by sophisticated computation in the brain. Knowledge of human motor control, which has been extensively studied in the fields of psychology and neuroscience, could play an important role in understanding the neural mechanism underlying adaptive driving behaviors (Lappi, 2015). However, a limited number of studies have investigated the neural basis for driving from the perspective of human motor control.

A neural system that may support flexible switching of driving modes is internal models, which mimic the input-output properties of our body or controlled devices (Wolpert et al., 1995; Wolpert and Kawato, 1998; Kawato, 1999). The brain maintains not a single but multiple internal models employed for different environments or properties of control devices. Previous neuroimaging studies suggest that the motor-related regions, especially in the cerebellum, maintain multiple internal models in a modular manner (Imamizu et al., 2003; Krakauer et al., 2004; Girgenrath et al., 2008). Imamizu et al. (2003) demonstrated that different control properties (velocity vs. rotation control of a computer mouse) were organized with spatially segregated patterns in the cerebellum. The neural mechanism that allows flexible switching of multiple internal models has also been studied (Imamizu et al., 2004; Imamizu and Kawato, 2008). The frontoparietal network (FPN) regions play a key role in internal model switching through interacting with the cerebellar cortex. The roles of the FPN regions are different; the superior parietal lobe (SPL) is involved in switching depending on predictive contextual information, while the dorsolateral prefrontal cortex (DLPFC) and inferior parietal lobe (IPL) contribute to switching driven by sensorimotor feedback (Imamizu and Kawato, 2008). Thus, the acquisition and switching of multiple internal models is fundamental to adaptive motor control. The previous literature on human motor control provides clues to understanding the neural mechanisms involved in flexible switching of driving modes in response to changes in the driving environment. However, previous findings were based on well-controlled experimental paradigms using a computer mouse or a joystick. It remains unknown whether the neural bases found in previous motor control studies also support the skills needed for practical car driving.

In the current study, we investigated the brain regions recruited in car driving using functional magnetic resonance imaging (fMRI). Participants drove a virtual car on a simulated circuit course by controlling custom-made devices, which had a relationship between device control and car behavior (i.e., input-output relationship in driving) similar to that in actual driving, inside the MRI scanner (**Figure 1A**). We defined the ratio of acceleration relative to a stepping-in amount of the accelerator pedal as accelerator sensitivity and abruptly changed this sensitivity at the mid-point of a straight section of the course in order to introduce unpredictable changes in the driving environment into the experimental task. Participants were required to respond to the change quickly while maintaining stable driving. We explored activation/deactivation in response

to the change in the level of accelerator sensitivity. We also performed multivoxel pattern analysis (MVPA) to examine the cerebellar activity patterns involved in switching of driving modes in response to different levels of accelerator sensitivity.

MATERIALS AND METHODS

Participants

Twenty-five healthy volunteers (three females) with a mean age of 21.9 years (19–33) participated in our experiment. We recruited volunteers who had obtained a driving license. The mean licensed period was 2.7 years (0.4–15). The mean hours of driving per week was 4.42 (0.25–21) across the participants. We collected data of 10 participants from the University of Tokyo and 15 participants from Hokkaido University. We excluded the data of five participants from analysis due to large head motion during the fMRI scan (for details, see below: *Preprocessing of MRI data*). We eventually analyzed the data of 20 participants (two females) with a mean age of 22.2 years (19–33), a mean licensed period of 2.9 years (0.8–15), and mean driving hours of 4.8 (0.5–21). Written informed consent was obtained from all volunteers in accordance with the latest version of the Declaration of Helsinki. The experimental protocol was approved by the ethics committee at the University of Tokyo.

Experimental Task

Participants drove a virtual car using a driving simulator (CarSim, Virtual Mechanics, Japan) by controlling a custom-made MRI-compatible control device (Leading-Edge Research and Development Accelerator, Inc., Japan; **Figure 1A**). They manipulated two levers serving as brake and accelerator pedals with their left hand while controlling a knob serving as a steering wheel with their right hand. This custom-made device required participants to coordinate different effectors to operate their virtual car, as with actual car driving. Furthermore, the input-output relationship in this virtual car driving was similar to that in actual driving. We customized program codes with MATLAB and Simulink (Mathworks, United States) to set up the ratio of acceleration/deceleration to a stepping-in amount of the brake and accelerator pedals and that of steering angle to the degree of turning the knob.

A virtual car ran on a circuit course consisting of 1,000-m straight sections and 150-m radius curves (**Figure 1B**). Participants were instructed to drive their car while following a preceding car during the task. They were required to keep their car at a 25-m distance from the preceding car as precisely as possible through the straight sections. We incorporated this task to control the timing of changes in accelerator sensitivity and participant driving behavior. Note that participants learned how to keep the target distance during the 5-day practice session before the fMRI experiment (for details, see below). Although following the preceding car was required, they were not required to attend to the distance between the two cars while driving through the curves. At the start of each run, the participant's car was placed at the beginning of a curve (star in **Figure 1B**). The preceding car ran at 40 km/h for the first 400 m of the straight

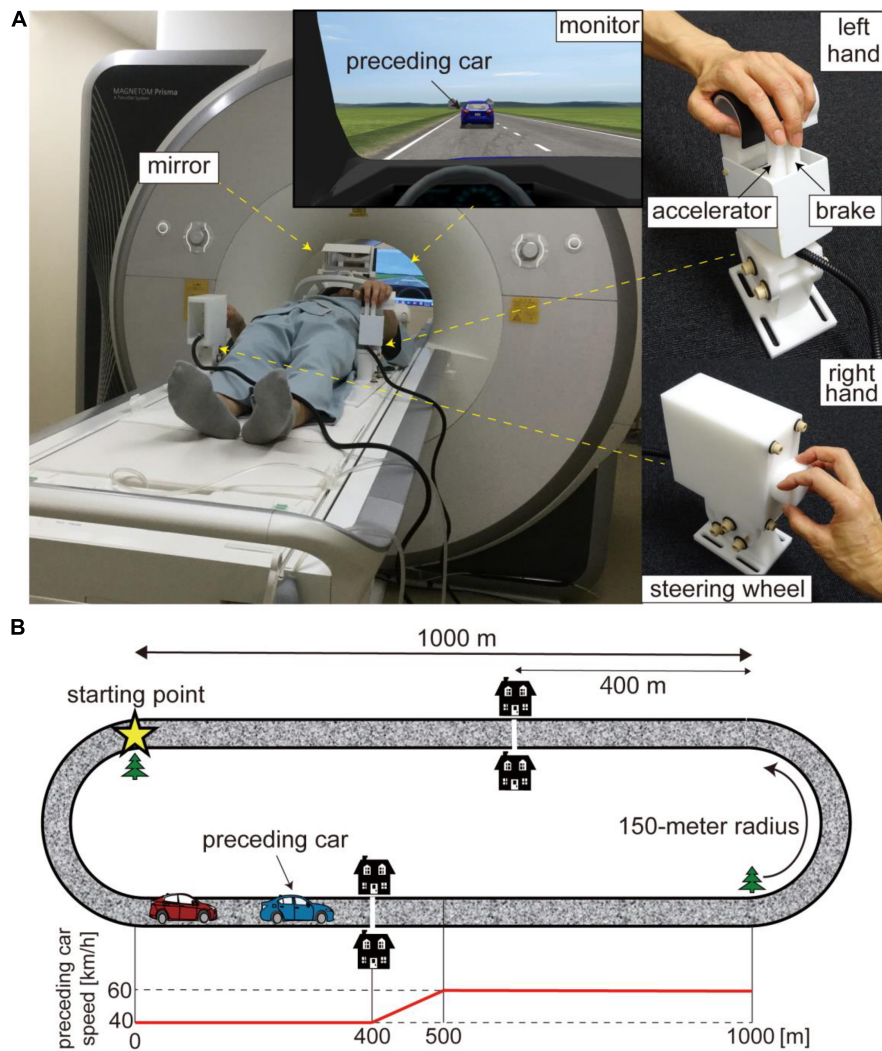


FIGURE 1 | (A) Experimental setup. Participants drove a virtual car while lying on the bed of an MRI scanner. The virtual car was controlled with MRI-compatible customized devices. The two levers manipulated with the index and middle fingers of the left hand served as brake and accelerator pedals (upper right) while the knob controlled with the right hand functioned as a steering wheel (lower right). Participants viewed a monitor via a mirror. **(B)** Driving course. The driving circuit consisted of 1,000-m straight sections and 150-m radius curves. The star denotes the starting point. The preceding car runs at 40 km/h for the first 400 m of the straight section and accelerates from 40 to 60 km/h for the next 100 m. The white line and two houses were displayed to inform participants of the acceleration point of the preceding car. The bottom panel shows the trajectory of the preceding car's speed. The trajectory is aligned to the beginning of the straight section (0 m).

section and accelerated from 40 to 60 km/h for the next 100 m. A white line across the road and two houses were located in the display 400 m from the beginning of the straight section to inform participants of the timing of the acceleration. Then, the preceding car ran on the remaining 500-m straight section at 60 km/h (speed trajectory of preceding car is shown in the bottom panel of **Figure 1B**, see also **Supplementary Movie 1**). We positioned a tree as a landmark of the end of the straight section. The preceding car decelerated from 60 to 40 km/h while going around a curve. We defined the drive through a straight section as one trial. Participants were asked to drive their car four laps in a run, that is, a run consisted of eight trials.

We defined “accelerator sensitivity” as the ratio of the acceleration of a virtual car to the stepping-in amount of

an accelerator pedal. We established two levels of accelerator sensitivity (high and low sensitivity), and they abruptly changed from one to the other in the middle of driving on the straight section. Specifically, they changed when the participant's car crossed the 500-m point from the beginning of the straight section. The high-sensitivity level was three times more sensitive than the low-sensitivity level. This means that a car at high sensitivity produced three times greater acceleration than one at low sensitivity with the same amount of stepping pressure on the accelerator pedal. The level of accelerator sensitivity changed in half of the trials, while not in the remainder of the trials. Participants were informed of the initial accelerator sensitivity at the beginning of each run to reduce the difficulty of driving through the first curve.

Experiment Schedule

We asked each participant to conduct a 5-day practice, held outside an MRI scanner, and a 2-day MRI session. Note that the practice and MRI sessions were not always conducted on consecutive days. One participant conducted MRI experiments for 3 days due to his limited schedule. In the practice session, participants drove their car with either low or high sensitivity during an entire run (i.e., without changes in accelerator sensitivity). They practiced driving a car with the two levels of sensitivity in eight runs each throughout the 5-day practice (i.e., 16 runs in total). We instructed them to keep a 25-m distance from the preceding car while driving. A white line was displayed 25 m behind the preceding car as guidance of the target distance in the first eight runs of the practice session. In addition to the 16-run practice, participants conducted the same task as the MRI experiment, in which the accelerator sensitivity changed in the middle of driving on a straight section, for two runs at the end of the practice session. The MRI session consisted of five runs per day, and thus we conducted 10 runs over 2 days. Note that three participants (out of 20) performed nine runs in total due to their limited schedule during the MRI scanning.

Magnetic Resonance Imaging Data Acquisition

A 3 Tesla Magnetom Prisma scanner (Siemens, Germany) with a 64-channel head coil was used to acquire T2*-weighted echo-planar images (EPI). We acquired 435 volumes in each run with a gradient echo EPI sequence under the following scanning parameters: repetition time (TR), 2,000 ms; echo time (TE), 30 ms; flip angle (FA), 80°; field of view (FOV), 192 × 192 mm; matrix, 64 × 64; 32 axial slices; and thickness, 4 mm with a 1-mm gap. T1-weighted (T1w) magnetization-prepared rapid acquisition gradient-echo (MP-RAGE) fine-structural images were obtained with 1 × 1 × 1-mm resolution with a gradient echo sequence [repetition time, 2,250 ms; echo time, 2.98 ms; inversion time (TI), 900 ms; flip angle, 9°; FOV, 256 × 256; 192 axial slices; and slice thickness, 1 mm without gap]. Although we collected MRI data at both the University of Tokyo and Hokkaido University, the scanners (i.e., 3 Tesla Magnetom Prisma, Siemens), number of channels in a coil, and imaging parameters were identical to each other.

Preprocessing of Magnetic Resonance Imaging Data

We performed preprocessing of the MRI data using the pipeline provided by fMRIPrep version 20.2.0 (Esteban et al., 2019). The preprocessing steps included slice-timing correction, motion correction, segmentation of T1-weighted structural images, coregistration, and normalization to Montreal Neurological Institute (MNI) space (for more details on the pipeline).¹ The first five volumes of each run were discarded. We next applied spatial smoothing to the data with a 6-mm full-width at half-maximum (FWHM) Gaussian kernel using SPM 12 (Wellcome Trust Centre for Neuroimaging, London, UCL) on MATLAB.

¹<http://fmriprep.readthedocs.io/en/latest/workflows.html>

Spatial smoothing was not applied to the data for MVPA, since this might blur the fine-grained information contained in multivoxel activity (Mur et al., 2009).

We calculated frame-wise displacement (FD) based on the six realign parameters as an index of the amount of head motion for each run in each participant (Power et al., 2012). We excluded the runs in which the number of frames with FD > 0.5 mm was over 5% of all frames in a run from further analysis. As a result, the number of runs of five participants' data became less than five; thus, we excluded these five participants from data analysis.

General Linear Model Analysis

We used a general linear model (GLM) analysis to explore activations or deactivations in brain regions after changing the level of accelerator sensitivity. One run included four conditions involving the sensitivity change: (1) change from low to high sensitivity, (2) change from high to low, (3) no change from low sensitivity, and (4) no change from high sensitivity. The following three periods of straight-section driving in each of the four conditions were modeled as separate 12-boxcar regressors that were convolved with a canonical hemodynamic response function: (1) a baseline period (period between the timings when the participant's car passed the 100-m point of the straight section and when the preceding car passed the 400-m point), (2) an acceleration period (period between the timings when the preceding car passed the 400-m point of the straight section and when the participant's car passed the 500-m point), (3) a target period (period between the timings when the participant's car passed the 500-m point of the straight section and when the preceding car passed the 1,000-m point). Note that we excluded the period for the first 100-m driving on the straight section from the baseline period to avoid contamination of the baseline period by the effect of curve driving. The six realign parameters were modeled as a regressor of no interest. We removed low-frequency noise using a high-pass filter with a cut-off period of 128 s. Serial correlations among scans were estimated with an autoregressive model implemented in SPM12.

To explore regions that were activated after the change in the level of accelerator sensitivity, we generated a contrast image using a fixed-effects model. We first generated contrasts of the target vs. baseline period in both the change and no-change conditions. We then subtracted the contrast in the no-change from that in the change condition:

$$(Target_c - Baseline_c) - (Target_n - Baseline_n). \quad (1)$$

Here, $Target_c$ and $Baseline_c$ represent the target and baseline periods, respectively, of the change condition. $Target_n$ and $Baseline_n$ represent the target and baseline periods, respectively, of the no-change condition. Next, we explored regions that were deactivated after the sensitivity change by subtracting the contrasts in the opposite direction:

$$(Target_n - Baseline_n) - (Target_c - Baseline_c). \quad (2)$$

We also generated contrasts of the acceleration vs. baseline period using trials in both change and no-change conditions together in order to investigate brain regions that were

activated or deactivated in response to acceleration of the preceding car. The contrast images of all participants were taken into the second-level group analysis using a random-effects model of a one-sample *t*-test. We adopted statistical inference with a threshold of $p < 0.05$ [family-wise error (FWE) corrected at cluster level with a cluster-forming threshold of $p < 0.001$]. The anatomical localization was determined according to the automated anatomical labeling (AAL) atlas (Tzourio-Mazoyer et al., 2002).

Multi-Voxel Pattern Analysis

We performed MVPA to classify whether participants were driving the car with either high or low accelerator sensitivity from the fMRI voxel patterns (Haynes and Rees, 2005; Kamitani and Tong, 2005; Norman et al., 2006). We modeled the target period of each of the eight trials as a separate boxcar regressor that was convolved with a canonical hemodynamic response function. The GLM also included the six realign parameters as a regressor of no interest. As a result, eight independently estimated parameters (β -values) per run were yielded for each voxel. We used the parameter estimates within a region of interest (ROI) as the input of a classifier. We used the linear support vector machine (SVM) implemented in LIBSVM² with default parameters (a fixed regularization parameter $C = 1$). Because it has been suggested that the cerebellum is involved in internal models (Shadmehr and Holcomb, 1997; Wolpert et al., 1998; Imamizu et al., 2000; Shadmehr and Krakauer, 2008; Cerminara et al., 2009; Stein, 2009), we targeted the anterior and posterior cerebellum as ROIs, which were anatomically defined with the AAL atlas and split into the left and right sides.

The SVM classifier was trained using the data in the no-change conditions (Figure 2, left). We first aimed to examine whether the cerebellar activity exhibited distinct patterns that corresponded to the low- and high-sensitivity levels. We thus applied the trained classifier to the data in the no-change conditions (“test 1” in Figure 2, right) and obtained a classification accuracy. Next, we aimed to examine whether the cerebellum switched its activity patterns according to the change in the level of accelerator sensitivity. Here, we applied the classifier trained with the data in the no-change condition to the data in the change conditions (“test 2” in Figure 2, right). Here, we allocated high- or low-sensitivity labels to the test data according to sensitivity levels after the sensitivity change (darker colored car in the bottom-right area of Figure 2). We expected classification accuracy to be significantly higher than chance level if voxel patterns were switched in response to the sensitivity change. In contrast, we expected classification accuracy to be significantly lower than chance if voxel patterns were unaffected by the change. We performed a leave-one-run-out cross-validation in both “test 1” and “test 2” procedures to estimate classification accuracies as a way to prevent the differences among runs from becoming a confounding factor.

We statistically tested decoding accuracies by calculating *z*-scores using the following permutation procedure (Langfelder et al., 2011; Shibata et al., 2016; Ohata et al., 2020). We

first randomly permuted the correspondence between the fMRI activity and the condition labels (i.e., high vs. low sensitivity) of the training dataset and then applied the classifier trained using the permuted data to the test dataset. We generated 1,000 surrogate classification accuracies by repeating the procedure 1,000 times. We calculated the *z*-scores of the original (without permutation) classification accuracies based on the empirical distribution of the 1,000 surrogate data for each participant separately. We tested the statistical significance of the *z*-scores using a two-sided *t*-test with a threshold of $p < 0.05$.

RESULTS

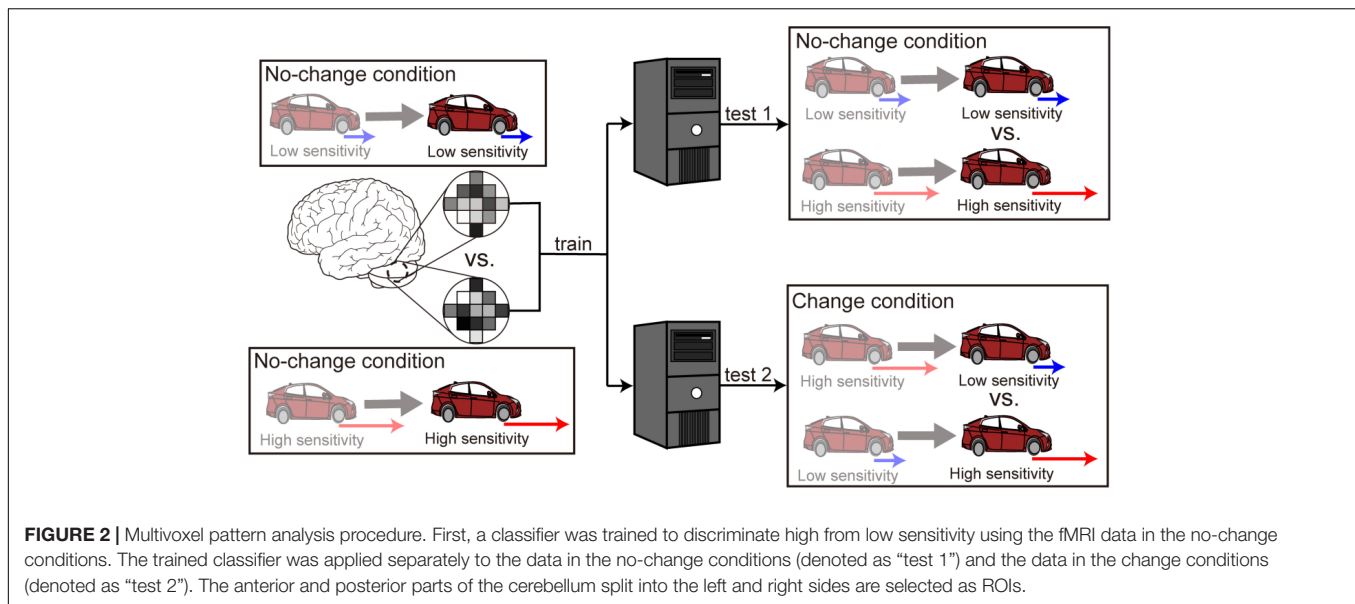
Behavioral Results

Figure 3A shows time courses of the inter-vehicle distance (distance between the preceding and participant's driving cars) for one participant as an example. The time courses were aligned at the possible timing of change in accelerator sensitivity (0 s: timing of passing the 500-m point of the straight section, see Figure 1B). His car speeded up after the change in the level of accelerator sensitivity from low to high, resulting in the shortened inter-vehicle distance (Figure 3A, left). By contrast, his car slowed down due to the sensitivity change from high to low, resulting in the lengthened distance (Figure 3A, right). Once the inter-vehicle distance reached the maximum or minimum, the distance gradually returned to the target distance (25 m). Next, we subtracted the inter-vehicle distance in the no-change condition from that in the change condition at every sampling point. Figure 3B shows the difference averaged across participants. The difference in the inter-vehicle distance became largest at 9.6 s (averaged across participants, SD: 4.5 s) after the accelerator sensitivity changed from low to high and at 12.0 s (SD: 6.0) after the sensitivity changed from high to low. Note that the reported mean peak timing is not the same as the peak timing seen in Figure 3B; this was because the averaged value was strongly affected by the data of some participants with large values.

General Linear Model Results

We explored the brain regions in which the activities responded to the change in the level of accelerator sensitivity according to the contrast of activity represented in Equation (1). Figure 4A shows the regions activated after the sensitivity change (see Table 1). We first found significant activation in the left cerebellum, cerebellar lobule VI. We also found activation in the bilateral supramarginal gyrus and right middle frontal gyrus, which are portions of the IPL and DLPFC, respectively. The bilateral anterior insula (AI) and the thalamus, which are the components of the salience network (SN, Seeley et al., 2007; Menon and Uddin, 2010; Seeley, 2019), also activated after the sensitivity change. Next, we explored the deactivations in response to the sensitivity change (Figure 4B and Table 1) according to the contrast represented in Eq. (2). The posterior cingulate cortex (PCC), which is a component of the default mode network (DMN, Raichle et al., 2001; Buckner et al., 2008), and a part of the right cerebellum (VIIA CrusI) were

²<http://www.csie.ntu.edu.tw/~cjlin/libsvm/>



significantly deactivated in response to the change in the level of accelerator sensitivity.

Next, we investigated brain regions activated by the acceleration of the preceding car. We generated the contrast between the acceleration and baseline periods from the data in both change and no-change conditions together. We found that some activated regions overlapped those found in **Figure 4** (**Supplementary Figure 1**). We were concerned that the activities involved in the preceding car’s acceleration were, for some reason, different between the change and no-change conditions and affected the activations in response to the change in sensitivity (i.e., **Figure 4**). To assess this concern, we generated the contrasts (acceleration vs. baseline periods) from the data in the change and no-change conditions separately. We compared the two contrasts but found no region showing a significant difference in the contrasts. Therefore, the activations/deactivations shown in **Figure 4** were very unlikely involved in the preceding car acceleration prior to the change in acceleration sensitivity. Finally, we compared the activation related to the accelerator sensitivity changes with those related to the preceding car’s acceleration. We found significantly larger activations in the sensorimotor regions, including the left primary motor area and supplementary motor area, and in the bilateral IPL in response to the preceding car’s acceleration than in response to the accelerator sensitivity changes (**Supplementary Figure 2**).

Multivoxel Pattern Analysis Results

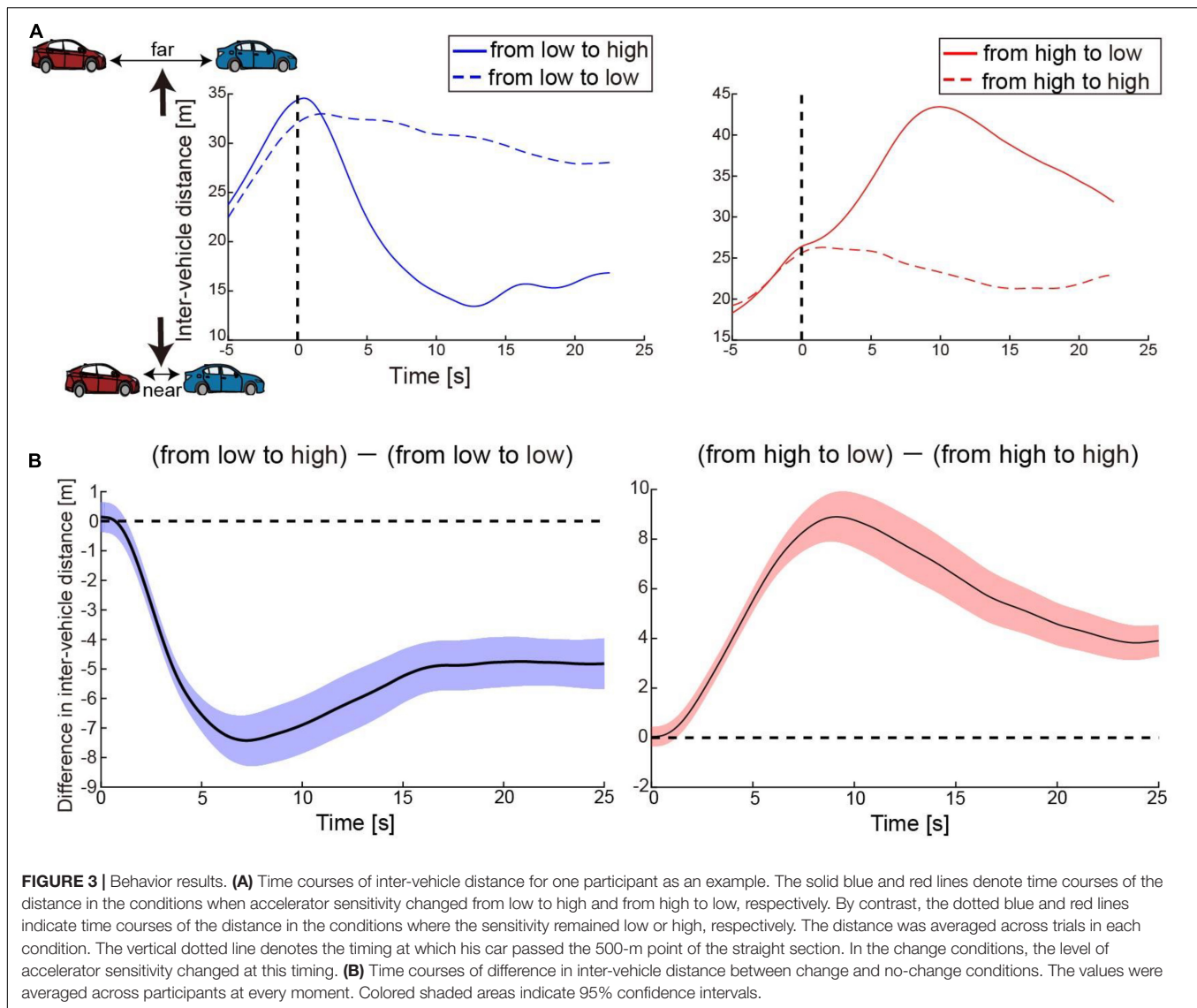
We first examined whether the cerebellar activity distinguished the two levels of accelerator sensitivity (high vs. low sensitivity) while participants were driving their car. We performed the classification analysis using the data only in the no-change condition (“test 1” in **Figure 2**). As a result, we did not find any significant above-chance classification accuracy in any cerebellar ROI: 50.6% (SD: 12.9%) in the left anterior cerebellum [$t(19) = -0.29, p = 0.77$], 48.9% (13.2%) in the right anterior

cerebellum [$t(19) = -0.31, p = 0.77$], 48.7% (11.5%) in the left posterior cerebellum [$t(19) = -0.50, p = 0.62$], and 52.5% (12.0%) in the right posterior cerebellum [$t(19) = 0.99, p = 0.33$]. We next applied the classifier trained using the data in the no-change condition to those in the change condition (“test 2” in **Figure 2**). The accuracy in no ROI was significantly higher than the chance level: 48.9% (7.02%) in the left anterior cerebellum [$t(19) = -0.74, p = 0.47$], 51.8% (7.03%) in the right anterior cerebellum [$t(19) = -0.97, p = 0.34$], 47.8% (8.76%) in the left posterior cerebellum [$t(19) = -1.26, p = 0.22$], and 51.5% (8.92%) in the right posterior cerebellum [$t(19) = 0.83, p = 0.42$]. Accordingly, contrary to our expectation, the cerebellum did not maintain distinct activity patterns corresponding to the two levels of accelerator sensitivity or switch patterns in response to the sensitivity change.

DISCUSSION

The current fMRI study investigated the neural bases supporting driving behaviors to flexibly switch driving modes in response to changes in the driving environment. We first found the activities in the sensorimotor area, including the cerebellum, the FPN, and SN regions, that increase in response to abrupt changes in the accelerator sensitivity of a virtual car (**Figure 4A**). By contrast, we found deactivation in the PCC, a component of the DMN, after the change (**Figure 4B**). The GLM results suggest that the sensorimotor system is engaged in adaptive behaviors for car driving. Our results also highlight the role of the large-scale networks related to saliency, attention, and cognition in adaptive driving behaviors.

Drivers are required to construct and switch multiple driving modes in response to changes in driving environments. Internal models may be the key mechanism underlying such adaptive driving behavior. Previous studies, in which participants controlled a computer mouse or joystick, demonstrated the



cerebellar activity that reflects the acquisition of internal models (Imamizu et al., 2000, 2003; Seidler and Noll, 2008; Kim et al., 2015). The current driving study also reveals that the activity in the left cerebellar lobule VI significantly increases after the change in the level of accelerator sensitivity (Figure 4A). Importantly, the activated area found in our study largely overlaps that involved in velocity control, not positional control, of a cursor manipulated with a computer mouse (Imamizu et al., 2003). This finding suggests the possibility that internal models for the same control property are allocated to the activity in the same cerebellar region regardless of the type of control device.

We also found activation in the DLPFC, IPL, and insula (Figure 4A), all of which were reported to be associated with internal model switching (Imamizu et al., 2004). It has been suggested that the DLPFC and IPL contribute to internal model switching driven by the error between predicted and actual sensorimotor feedback (postdictive switching, Imamizu and Kawato, 2008). Forward internal models predict sensorimotor

feedback from the efference copy of a motor command and are influential in the comparison between predicted and actual feedback (Wolpert et al., 1995; Miall and Wolpert, 1996; Blakemore et al., 2000). In our task, the level of accelerator sensitivity randomly changed in a trial-by-trial manner so that internal models could not be switched in advance of the sensitivity change (i.e., predictive switching). Thus, the model optimized for the environment before the sensitivity change addressed the new environment, resulting in a large prediction error. Our results suggest that such prediction error functioned as a signal of the change in the driving environment and prompted the brain to switch internal models postdictively.

Although the GLM results suggest the possibility of internal model switching, the MVPA results show neither distinction nor switching of cerebellar activity patterns during car driving. One possible reason for this unexpected result is that internal model switching is not necessarily an optimal strategy for every participant to address changes in the driving environment.

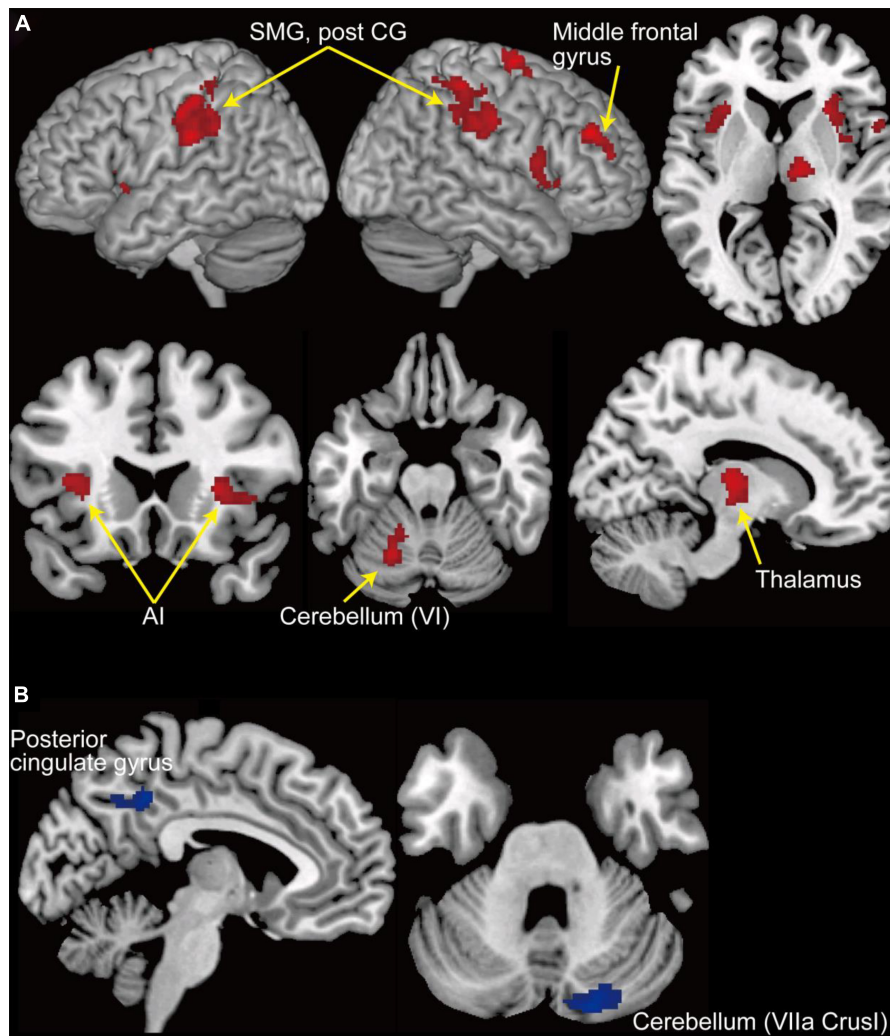


FIGURE 4 | GLM results. **(A)** Clusters of activation (in red) that significantly increased after change in the level of accelerator sensitivity. **(B)** Clusters of activation (in blue) that significantly decreased after change in the level of accelerator sensitivity. A threshold at $p < 0.05$ (FWE-corrected at cluster level with a cluster-forming threshold of $p < 0.001$) was set for statistical testing. AI, anterior insula; Post CG, post central gyrus; SMG, supramarginal gyrus.

Driving engages executive cognitive functions, such as attentional control, cognitive inhibition, and cognitive flexibility (Navarro et al., 2018). Some participants might dominantly exert cognitive strategies in which such executive functions are employed rather than internal model switching. The driving simulator used in this study did not provide a perfectly realistic driving experience. The difference between real and simulated driving experiences might encourage participants to develop cognitive strategies uniquely optimal to the simulated environment. We found a large variance in the classification accuracies across participants, which might imply individual differences in their strategies. Another possible reason is the difficulty of controlling participant driving behavior in the driving simulator. We could control participant driving behavior to some extent by requiring them to follow the preceding car at a constant distance. However, there was no measure to monitor whether and when participants switched their driving modes. Hence, it might be possible to use the trials

in which participants could not switch their driving modes, or the switching timing was much delayed, for MVPA.

We also found deactivation in the PCC in response to the change in the level of accelerator sensitivity (**Figure 4B**). The PCC is a part of the DMN, a set of coordinated brain regions that shows more activation at rest than during cognitive demand tasks (Raichle et al., 2001; Buckner et al., 2008). The DMN regions respond to non-stimulus induced or internally oriented thoughts such as mind-wandering (Andrews-Hanna et al., 2010; Raichle, 2015), and thus the activation could interfere with task performance (Eichele et al., 2008; Hinds et al., 2013). The change in the driving environment possibly required participants to switch their cognitive modes of car-driving in addition to internal model switching. The deactivation in the PCC encouraged them to switch such cognitive modes quickly. The activities in the DMN regions are typically anticorrelated to those in the FPN regions (Fox et al., 2005, 2009). Previous studies suggest the

TABLE 1 | Summary of GLM results.

Brain region	Side	Cluster size	t-value at peak	MNI coordinates(Peak voxel)		
				x	y	z
Activate						
1. Thalamus	Right	282	6.53	16	-16	12
2. Supramarginal gyrus	Left	647	6.06	-66	-26	28
3. Superior frontal gyrus	Right	208	6.05	24	-4	72
4. Middle frontal gyrus	Right	156	6.00	36	40	32
5. Postcentral gyrus	Right	624	5.91	38	-34	58
6. Cerebellum (VI)	Left	190	5.46	-20	-60	-22
7. Insula	Right	290	5.14	28	20	6
8. Insula	Left	204	4.94	-30	16	12
9. Opercular part of inferior frontal gyrus	Right	144	4.71	54	10	14
Deactivate						
1. Cerebellum (VIIa Crus1)	Right	252	6.21	16	-84	-34
2. Posterior cingulate gyrus	Left	158	5.00	-2	-44	42

A threshold at $p < 0.05$ (FWE-corrected at cluster level with a cluster-forming threshold of $p < 0.001$) was set for statistical testing.

crucial role of the SN in switching this balance between the FPN and DMN (Sridharan et al., 2008; Menon and Uddin, 2010; Uddin, 2015). Importantly, the current study found significant activation in the bilateral AI and thalamus, parts of the SN (**Figure 4A**). Our results imply the involvement of the large-scale networks (FPN, DMN, and SN) and their switching mechanism in adaptive driving behavior, which was a possible candidate of unique neural features for car driving.

Previous neuroimaging studies have identified multiple brain regions involved in different aspects of car driving using driving simulators or video games (Walter et al., 2001; Calhoun et al., 2002; Uchiyama et al., 2003; Horikawa et al., 2005; Spiers and Maguire, 2007; Okamoto et al., 2020; see also review and meta-analysis studies in Lappi, 2015; Navarro et al., 2018). The neural correlates of driving reported in the previous literature overlap those found in the current study. Calhoun et al. (2002), having identified functional co-activation patterns using independent component analysis, related the cerebellar and occipital activation to complex visuomotor integration during driving. This study also found that the activation in the DMN regions decreased during driving and was negatively correlated with driving speed, suggesting an association with the vigilance function during driving. In addition, Spiers and Maguire (2007) suggested that the activations in the cerebellum, posterior parietal cortex, and SN regions were associated with unprepared actions such as swerving and avoiding collisions. These regions were considered necessary for responding to abrupt events. Thus, the brain regions found in the current study reflected the suggestions from previous findings. Meanwhile, our study aimed at more specific functions for driving (i.e., switching of multiple driving modes) than those examined in previous studies in order to elucidate the detailed role of each region from the perspective of adaptive motor control.

Although we obtained findings suggesting that adaptive driving behaviors were involved in internal model switching,

it is still open to debate whether the brain allocates different internal models to different parameters with the same type of control property (e.g., different angles in rotation control or different gains in velocity control). Hence, there remains the possibility that the brain achieved switching of driving mode without changing internal models in the current experimental setting. One possible scenario could be the brain using a single internal model for controlling a virtual car and adjusting the control parameters of the internal model in response to changes in the driving environment. Consequently, as a limitation of this study, we cannot deny the possibility that the internal models are not switched.

As mentioned above, our driving simulator cannot represent a perfectly realistic driving experience. In particular, the device used in this study required participants to control steering and acceleration/deceleration using different effectors from those used in actual driving (i.e., steering control by turning a steering knob with the right hand vs. by manipulating a steering wheel with both hands; acceleration/brake control by pushing two pedals with the left index finger vs. by stepping on two pedals with the right foot). We assume that the skill targeted in the current study, that is, flexibly switching different driving modes in response to changes in the driving environment, is supported by higher-order motor/cognitive functions that can be generalized regardless of the effectors used. However, we still cannot deny the possibility that the target skill is dependent on control devices. Therefore, it might also be possible that we observed brain activities that were unique to the current setup. The best approach to overcoming this limitation is to develop a device that can measure brain activity, with comparable precision to an fMRI scanner, in a real car. Because the current technology cannot offer such devices, we translated driving behaviors into possible naturalistic behaviors inside an fMRI scanner while minimizing head movements (realistic steering handle and acceleration and brake pedals manipulated in the MRI environment;

Kim et al., 2020; Okamoto et al., 2020). In our simulator, the accelerator and brake pedals were replaced by hand levers while the steering wheel was replaced by a knob dial. Such substitutions are common in the controllers of remote-control cars. Future studies are needed to improve both the driving simulator and neuroimaging devices in order to measure brain activities in more realistic driving experiences than that of the current study.

The current study targeted adaptive driving behaviors determined by sensorimotor feedback (i.e., switching of driving modes in response to changes in the driving environment postdictively). However, experienced drivers also possess the skill of anticipating future changes and preparing for possible responses to environmental changes. Unfortunately, our experimental design did not allow us to investigate such predictive aspects of driving skills. To further probe comprehensive driving skills, we need future studies on predictive switching of driving modes by introducing into experimental tasks various environmental changes that participants can anticipate in advance (e.g., an uphill incline that decelerates car speed).

In sum, this study searched for the neural substrates that support flexibly switching of different driving modes in car driving. Our findings demonstrate that the neural bases found in previous motor control studies, especially the cerebellum involving internal models and the DLPFC, IPL, and insula for switching of different internal models, are also fundamental to the adaptive behaviors of switching driving modes. Furthermore, this study also highlighted the involvement of the large-scale brain network in addressing cognitive demands for driving, suggesting a possible neural process unique to car driving.

DATA AVAILABILITY STATEMENT

The raw data supporting the conclusions of this article will be made available by the authors, without undue reservation.

REFERENCES

- Andrews-Hanna, J. R., Reidler, J. S., Huang, C., and Buckner, R. L. (2010). Evidence for the default network's role in spontaneous cognition. *J. Neurophysiol.* 104, 322–335. doi: 10.1152/jn.00830.2009
- Blakemore, S. J., Wolpert, D., and Frith, C. (2000). Why can't you tickle yourself? *Neuroreport* 11, R11–R16. doi: 10.1097/00001756-200008030-00002
- Buckner, R. L., Andrews-Hanna, J. R., and Schacter, D. L. (2008). The brain's default network: anatomy, function, and relevance to disease. *Ann. N. Y. Acad. Sci.* 1124, 1–38. doi: 10.1196/annals.1440.011
- Calhoun, V. D., Pekar, J. J., McGinty, V. B., Adali, T., Watson, T. D., and Pearlson, G. D. (2002). Different activation dynamics in multiple neural systems during simulated driving. *Hum. Brain Mapp.* 16, 158–167. doi: 10.1002/hbm.10032
- Cerminara, N. L., Apps, R., and Marple-Horvat, D. E. (2009). An internal model of a moving visual target in the lateral cerebellum. *J. Physiol.* 587, 429–442. doi: 10.1113/jphysiol.2008.163337
- Eichele, T., Debener, S., Calhoun, V. D., Specht, K., Engel, A. K., Hugdahl, K., et al. (2008). Prediction of human errors by maladaptive changes in event-related brain networks. *Proc. Natl. Acad. Sci. U.S.A.* 105, 6173–6178. doi: 10.1073/pnas.0708965105
- Esteban, O., Markiewicz, C. J., Blair, R. W., Moodie, C. A., Isik, A. I., Erramuzpe, A., et al. (2019). fMRIPrep: a robust preprocessing pipeline

ETHICS STATEMENT

The studies involving human participants were reviewed and approved by The University of Tokyo. The patients/participants provided their written informed consent to participate in this study.

AUTHOR CONTRIBUTIONS

RO and HI designed the study and wrote the manuscript. RO and KO collected the data. RO analyzed the data. KO reviewed and approved the final version of the manuscript. All authors contributed to the article and approved the submitted version.

FUNDING

This study was supported by a TOYOTA Joint Research Grant. HI was partially supported by JSPS KAKENHI (Grant Nos. 19H05725 and 21H03780).

ACKNOWLEDGMENTS

We are grateful to Terumasa Endo, Satoshi Inoue, and Takeshi Hamaguchi (TOYOTA Motor Corporation) for their help in the experimental setup and insightful discussions about the results. We also thank Shuhei Nishida and Yusuke Haruki for their assistance in collecting the data.

SUPPLEMENTARY MATERIAL

The Supplementary Material for this article can be found online at: <https://www.frontiersin.org/articles/10.3389/fnhum.2022.788729/full#supplementary-material>

- for functional MRI. *Nat. Methods* 16, 111–116. doi: 10.1038/s41592-018-0235-4
- Fox, M. D., Snyder, A. Z., Vincent, J. L., Corbetta, M., Van Essen, D. C., and Raichle, M. E. (2005). The human brain is intrinsically organized into dynamic, anticorrelated functional networks. *Proc. Natl. Acad. Sci. U.S.A.* 102, 9673–9678. doi: 10.1073/pnas.0504136102
- Fox, M. D., Zhang, D., Snyder, A. Z., and Raichle, M. E. (2009). The global signal and observed anticorrelated resting state brain networks. *J. Neurophysiol.* 101, 3270–3283. doi: 10.1152/jn.90777.2008
- Girgenrath, M., Bock, O., and Seitz, R. J. (2008). An fMRI study of brain activation in a visual adaptation task: activation limited to sensory guidance. *Exp. Brain Res.* 184, 561–569. doi: 10.1007/s00221-007-1124-8
- Haynes, J. D., and Rees, G. (2005). Predicting the orientation of invisible stimuli from activity in human primary visual cortex. *Nat. Neurosci.* 8, 686–691. doi: 10.1038/nn1445
- Hinds, O., Thompson, T. W., Ghosh, S., Yoo, J. J., Whitfield-Gabrieli, S., Triantafyllou, C., et al. (2013). Roles of default-mode network and supplementary motor area in human vigilance performance: evidence from real-time fMRI. *J. Neurophysiol.* 109, 1250–1258. doi: 10.1152/jn.00533.2011
- Horikawa, E., Okamura, N., Tashiro, M., Sakurada, Y., Maruyama, M., Arai, H., et al. (2005). The neural correlates of driving performance identified using

- positron emission tomography. *Brain Cogn.* 58, 166–171. doi: 10.1016/j.bandc.2004.10.002
- Imamizu, H., and Kawato, M. (2008). Neural correlates of predictive and postdictive switching mechanisms for internal models. *J. Neurosci.* 28, 10751–10765. doi: 10.1523/JNEUROSCI.1106-08.2008
- Imamizu, H., Kuroda, T., Miyauchi, S., Yoshioka, T., and Kawato, M. (2003). Modular organization of internal models of tools in the human cerebellum. *Proc. Natl. Acad. Sci. U.S.A.* 100, 5461–5466. doi: 10.1073/pnas.0835746100
- Imamizu, H., Kuroda, T., Yoshioka, T., and Kawato, M. (2004). Functional magnetic resonance imaging examination of two modular architectures for switching multiple internal models. *J. Neurosci.* 24, 1173–1181. doi: 10.1523/JNEUROSCI.4011-03.2004
- Imamizu, H., Miyauchi, S., Tamada, T., Sasaki, Y., Takino, R., Putz, B., et al. (2000). Human cerebellar activity reflecting an acquired internal model of a new tool. *Nature* 403, 192–195. doi: 10.1038/35003194
- Kamitani, Y., and Tong, F. (2005). Decoding the visual and subjective contents of the human brain. *Nat. Neurosci.* 8, 679–685. doi: 10.1038/nn1444
- Kawato, M. (1999). Internal models for motor control and trajectory planning. *Curr. Opin. Neurobiol.* 9, 718–727. doi: 10.1016/s0959-4388(99)00028-8
- Kim, H. S., Mun, K. R., Choi, M. H., and Chung, S. C. (2020). Development of an fMRI-compatible driving simulator with simultaneous measurement of physiological and kinematic signals: the multi-biosignal measurement system for driving (MMSD). *Technol. Health Care* 28, 335–345. doi: 10.3233/THC-209034
- Kim, S., Ogawa, K., Lv, J., Schweighofer, N., and Imamizu, H. (2015). Neural substrates related to motor memory with multiple timescales in sensorimotor adaptation. *PLoS Biol.* 13:e1002312. doi: 10.1371/journal.pbio.1002312
- Krakauer, J. W., Ghilardi, M. F., Mentis, M., Barnes, A., Veytsman, M., Eidelberg, D., et al. (2004). Differential cortical and subcortical activations in learning rotations and gains for reaching: a PET study. *J. Neurophysiol.* 91, 924–933. doi: 10.1152/jn.00675.2003
- Langfelder, P., Luo, R., Oldham, M. C., and Horvath, S. (2011). Is my network module preserved and reproducible? *PLoS Comput. Biol.* 7:e1001057. doi: 10.1371/journal.pcbi.1001057
- Lappi, O. (2015). The racer's brain—how domain expertise is reflected in the neural substrates of driving. *Front. Hum. Neurosci.* 9:635. doi: 10.3389/fnhum.2015.00635
- Menon, V., and Uddin, L. Q. (2010). Saliency, switching, attention and control: a network model of insula function. *Brain Struct. Funct.* 214, 655–667. doi: 10.1007/s00429-010-0262-0
- Miall, R. C., and Wolpert, D. M. (1996). Forward models for physiological motor control. *Neural Netw.* 9, 1265–1279. doi: 10.1016/S0893-6080(96)00035-4
- Mur, M., Bandettini, P. A., and Kriegeskorte, N. (2009). Revealing representational content with pattern-information fMRI—an introductory guide. *Soc. Cogn. Affect. Neurosci.* 4, 101–109. doi: 10.1093/scan/nsn044
- Navarro, J., Reynaud, E., and Osiurak, F. (2018). Neuroergonomics of car driving: a critical meta-analysis of neuroimaging data on the human brain behind the wheel. *Neurosci. Biobehav. Rev.* 95, 464–479. doi: 10.1016/j.neubiorev.2018.10.016
- Norman, K. A., Polyn, S. M., Detre, G. J., and Haxby, J. V. (2006). Beyond mind-reading: multi-voxel pattern analysis of fMRI data. *Trends Cogn. Sci.* 10, 424–430. doi: 10.1016/j.tics.2006.07.005
- Ohata, R., Asai, T., Kadota, H., Shigemasa, H., Ogawa, K., and Imamizu, H. (2020). Sense of agency beyond sensorimotor process: decoding self-other action attribution in the human brain. *Cereb. Cortex* 30, 4076–4091. doi: 10.1093/cercor/bhaa028
- Okamoto, Y., Sasaoka, T., Sadato, N., Fukunaga, M., Yamamoto, T., Soh, Z., et al. (2020). Is human brain activity during driving operations modulated by the viscoelastic characteristics of a steering wheel?: An fMRI study. *IEEE Access* 8, 215073–215090. doi: 10.1109/access.2020.3040231
- Power, J. D., Barnes, K. A., Snyder, A. Z., Schlaggar, B. L., and Petersen, S. E. (2012). Spurious but systematic correlations in functional connectivity MRI networks arise from subject motion. *Neuroimage* 59, 2142–2154. doi: 10.1016/j.neuroimage.2011.10.018
- Raichle, M. E. (2015). The brain's default mode network. *Annu. Rev. Neurosci.* 38, 433–447. doi: 10.1146/annurev-neuro-071013-014030
- Raichle, M. E., MacLeod, A. M., Snyder, A. Z., Powers, W. J., Gusnard, D. A., and Shulman, G. L. (2001). A default mode of brain function. *Proc. Natl. Acad. Sci. U.S.A.* 98, 676–682. doi: 10.1073/pnas.98.2.676
- Seeley, W. W. (2019). The salience network: a neural system for perceiving and responding to homeostatic demands. *J. Neurosci.* 39, 9878–9882. doi: 10.1523/jneurosci.1138-17.2019
- Seeley, W. W., Menon, V., Schatzberg, A. F., Keller, J., Glover, G. H., Kenna, H., et al. (2007). Dissociable intrinsic connectivity networks for salience processing and executive control. *J. Neurosci.* 27, 2349–2356. doi: 10.1523/JNEUROSCI.5587-06.2007
- Seidler, R. D., and Noll, D. C. (2008). Neuroanatomical correlates of motor acquisition and motor transfer. *J. Neurophysiol.* 99, 1836–1845. doi: 10.1152/jn.01187.2007
- Shadmehr, R., and Holcomb, H. H. (1997). Neural correlates of motor memory consolidation. *Science* 277, 821–825. doi: 10.1126/science.277.5327.821
- Shadmehr, R., and Krakauer, J. W. (2008). A computational neuroanatomy for motor control. *Exp. Brain Res.* 185, 359–381. doi: 10.1007/s00221-008-1280-5
- Shibata, K., Watanabe, T., Kawato, M., and Sasaki, Y. (2016). Differential activation patterns in the same brain region led to opposite emotional states. *PLoS Biol.* 14:e1002546. doi: 10.1371/journal.pbio.1002546
- Spiers, H. J., and Maguire, E. A. (2007). Neural substrates of driving behaviour. *Neuroimage* 36, 245–255. doi: 10.1016/j.neuroimage.2007.02.032
- Sridharan, D., Levitin, D. J., and Menon, V. (2008). A critical role for the right fronto-insular cortex in switching between central-executive and default-mode networks. *Proc. Natl. Acad. Sci. U.S.A.* 105, 12569–12574. doi: 10.1073/pnas.0800005105
- Stein, J. (2009). Cerebellar forward models to control movement. *J. Physiol.* 587, 299–299. doi: 10.1113/jphysiol.2008.167627
- Tzourio-Mazoyer, N., Landeau, B., Papathanassiou, D., Crivello, F., Etard, O., Delcroix, N., et al. (2002). Automated anatomical labeling of activations in SPM using a macroscopic anatomical parcellation of the MNI MRI single-subject brain. *Neuroimage* 15, 273–289. doi: 10.1006/nimg.2001.0978
- Uchiyama, Y., Ebe, K., Kozato, A., Okada, T., and Sadato, N. (2003). The neural substrates of driving at a safe distance: a functional MRI study. *Neurosci. Lett.* 352, 199–202. doi: 10.1016/j.neulet.2003.08.072
- Uddin, L. Q. (2015). Saliency processing and insular cortical function and dysfunction. *Nat. Rev. Neurosci.* 16, 55–61. doi: 10.1038/nrn3857
- Walter, H., Vetter, S. C., Grothe, J., Wunderlich, A. P., Hahn, S., and Spitzer, M. (2001). The neural correlates of driving. *Neuroreport* 12, 1763–1767. doi: 10.1097/00001756-200106130-00049
- Wolpert, D. M., Ghahramani, Z., and Jordan, M. I. (1995). An internal model for sensorimotor integration. *Science* 269, 1880–1882. doi: 10.1126/science.7569931
- Wolpert, D. M., and Kawato, M. (1998). Multiple paired forward and inverse models for motor control. *Neural Netw.* 11, 1317–1329. doi: 10.1016/s0893-6080(98)00066-5
- Wolpert, D. M., Miall, R. C., and Kawato, M. (1998). Internal models in the cerebellum. *Trends Cogn. Sci.* 2, 338–347. doi: 10.1016/S1364-6613(98)01221-2

Conflict of Interest: The authors declare that this study received funding from TOYOTA. The funder had the following involvement in the study: discussions about the experimental setup and the results.

Publisher's Note: All claims expressed in this article are solely those of the authors and do not necessarily represent those of their affiliated organizations, or those of the publisher, the editors and the reviewers. Any product that may be evaluated in this article, or claim that may be made by its manufacturer, is not guaranteed or endorsed by the publisher.

Copyright © 2022 Ohata, Ogawa and Imamizu. This is an open-access article distributed under the terms of the Creative Commons Attribution License (CC BY). The use, distribution or reproduction in other forums is permitted, provided the original author(s) and the copyright owner(s) are credited and that the original publication in this journal is cited, in accordance with accepted academic practice. No use, distribution or reproduction is permitted which does not comply with these terms.